Electronic Supplementary Material (ESI) for Inorganic Chemistry Frontiers.

# Luminescent vapochromic single crystal to single crystal transition in one-dimensional coordination polymer featuring the first Cu(I) dimer bridged by an aqua ligand.

Sloane Evariste, Ali Moustafa Khalil, Sebastien Kerneis, Chendong Xu, Guillaume Calvez,* Karine Costuas* and Christophe Lescop*

Institut des Sciences Chimiques de Rennes, CNRS - INSA - Université de Rennes 1, Campus de Beaulieu, 35042 Rennes Cedex, France.

**Supporting Information**

## Table of contents

# I. Experimental Section

For the preparation of the polymer **D**, procedures were performed under air, in a simple flask. Commercially available solvents were used as received without further purification. Commercially available reagents ([Cu($CH_3CN$)$_4$].$PF_6$, dppm, and 1,4-dicyanobenzene ligand $\mathbf{B_0}$ were obtained from Sigma-Aldrich. $^1$H and $^{31}$P{$^1$H} NMR spectra were recorded on Bruker AV300 or AV400 spectrometers. $^1$H NMR chemical shifts were reported in parts per million (ppm) relative to $Me_4Si$ as external standard. $^{31}$P{$^1$H} NMR downfield chemical shifts were expressed with a positive sign, in ppm, relative to 85% $H_3PO_4$ respectively. FT-IR measurements have been performed on a Perkin Elmer Frontier spectrometer using UATR (Universal Attenuated Total Reflectance) accessory. Spectra have been recorded between 650 $cm^{-1}$ and 4000 $cm^{-1}$, on pure samples. UV-vis solid-state absorption measurements have been recorded on a Perkin-Elmer Lambda 650 spectrometer using a 60 mm integrating sphere. Spectra have been recorded between 800 nm and 200 nm, on pellets.

Steady-state emission spectra and luminescence quantum yield measurements were recorded on a *Horiba Jobin-Yvon* (*HJY*) Fluorolog-3 (FL3-2iHR550) fluorescence spectrofluorometer equipped with a IR R928P PMT / *HJY* FL-1073 detector and with an integrating sphere. Low temperature measurements were allowed by using a OptistatCF (*Oxford Inst.*) in the range of 77 K to 300 K. Excited-state lifetimes in the range 80 K and 300 K were measured with a delta hub (TCSPC: Time-Correlated-Single-Photon-Counting) + delta diode system allowing to measure excited-state lifetimes between 500 ps et 10 µs and with a pulsed xenon source (FL-1035) allowing to measure excited-state lifetimes longer than 10 µs.

Solid sample was placed in a quartz sample holders inside the integrating sphere and the cryostat and maintained at the desired temperature until equilibrium was reached before recording the spectrum.

**Synthesis of derivative $\mathbf{D_{dry}}$**

One equivalent of 1,4-dicyanobenzene (0.007 g, 0.052 mmol) ligand $\mathbf{B_0}$ was added to one equivalent of the [$Cu_2$($\mu_2$-dppm)$_2$($CH_3CN$)$_4$]($PF_6$)$_2$ complex **A** prepared in-situ in $CH_2Cl_2$ at room temperature from the reaction of [Cu($CH_3CN$)$_4$]($PF_6$) (0.039 g, 0.104 mmol) and dppm (0.040 g, 0.104 mmol). To this clear solution were added

200 µL of distillated water. The resulting reaction mixture was stirred overnight at room temperature. The crude solution was then left upon pentane vapour diffusion, affording after one week of crystallization colourless single crystals. They were collected through filtration and dried under vacuum affording the derivative $\mathbf{D_{dry}}$ (0.055 g, 0.040 mmol, 80% yield) as an air-stable colourless polycrystalline solid.

Solution NMR data were obtained by dissolving crystals of $\mathbf{D_{dry}}$ in dry $CD_2Cl_2$:

$^1$H NMR (300 MHz, $CD_2Cl_2$): δ = 3.33 – 3.44 (m, 4H, P$CH_2$P), 6.98 (t, 8H, J = 7.5 Hz, $H_{dppm}$ in the *para* position relative to the phosphorus atom), 7.18 (t, 16H, J = 7.7 Hz, *meta* $H_{dppm}$), 7.32 (d, 16H, J = 7.1 Hz, *ortho* $H_{dppm}$), 7.79 (s, 4H, protons of the 1,4-dicyanobenzene).

$^{31}P\{^1H\}$ NMR (121 MHz, $CD_2Cl_2$): δ = -8.8 (broad s), -150.0 (sept., $PF_6^-$).

IR (cm$^{-1}$): 697 (vs), 739 (vs), 823(vs), 1097(s), 1260 (w), 1438 (w), 1486 (w), 2253 ($\upsilon_{CN}$, vw), 2958 (vw), 3057 (w), 3646 ($\upsilon_{OH}$, vw)

Elemental analysis, calcd. (%) for $C_{58}H_{50}O_1Cu_2F_{12}N_2P_6$: C 52.30, H 3.78, N 2.10; found: C 51.86, H 3.66, N 1.95.

### Preparation of derivatives $\mathbf{D_{CH2Cl2}}$, $\mathbf{D_{EtOH}}$, $\mathbf{D_{CH3NO2}}$ and $\mathbf{D_{THF}}$

Typical procedure consisted by placing single crystals of $\mathbf{D_{dry}}$ in the suitable sample holder considering the measurement subsequently conducted. This sample holder was put in an empty beaker that, in turn, was placed in a larger beaker containing a few mL of the considered solvant ($CH_2Cl_2$, EtOH, $CH_3NO_2$ or THF). This second beaker was covered and left at room temperature for 5 mn. After this lap of time, it was possible to apply a UV light irradiation at $\lambda_{ex}$ = 365 nm to observe that the initial eye-perceived blue-cyan solid state luminescence of **Ddry** was converted to an eye-perceived green to yellow solid state solid state luminescence typical of the solvated crystal of $\mathbf{D_{CH2Cl2}}$, $\mathbf{D_{EtOH}}$, $\mathbf{D_{CH3NO2}}$ or $\mathbf{D_{THF}}$.

The sample holder was then collected, closed and immediately adapted to the targeted characterisation device on which we checked that, before and after the measurement by applying a UV light irradiation at $\lambda_{ex}$ = 365 nm, the initial green to yellow solid state luminescence typical of the solvated crystal of $\mathbf{D_{CH2Cl2}}$, $\mathbf{D_{EtOH}}$, $\mathbf{D_{CH3NO2}}$ or $\mathbf{D_{THF}}$ was still observed.

## II. X-ray Crystallographic Study

Single crystal data collection for $\mathbf{D_{dry}}$, $\mathbf{D_{CH2Cl2}}$, $\mathbf{D_{EtOH}}$, $\mathbf{D_{CH3NO2}}$ and $\mathbf{D_{THF}}$. were performed at 150 K with a D8 Venture Bruker AXS (Centre de Diffractométrie, Université de Rennes 1, France) with Mo-$K\alpha$ radiation ($\lambda$ = 0.71073 Å). Reflections were indexed, Lorentz-polarization corrected and integrated by the *DENZO* program of the KappaCCD software package. The data merging process was performed using the SCALEPACK program.[1] Structure determinations were performed by direct methods with the solving program SIR97,[2] that revealed all the non-hydrogen atoms. SHELXL program[3] was used to refine the structures by full-matrix least-squares based on $F^2$. All non-hydrogen atoms were refined with anisotropic displacement parameters. Unless specifically mentioned (*vide infra*) in the detailed description of each different X-ray crystal structure resolutions, hydrogen atoms were included in idealised positions and refined with isotropic displacement parameters.

Single crystals of all these derivatives were always coated in paratone oil, mounted at low temperature on the diffractometer goniometer as quickly as possible in the case of the solvated crystals $\mathbf{D_{CH2Cl2}}$, $\mathbf{D_{EtOH}}$, $\mathbf{D_{CH3NO2}}$ and $\mathbf{D_{THF}}$) and X-ray data collection were performed at low temperature.

Upon the vapochromic single crystal to single crystal transition from $\mathbf{D_{dry}}$ to $\mathbf{D_{CH2Cl2}}$, $\mathbf{D_{EtOH}}$, $\mathbf{D_{CH3NO2}}$ or $\mathbf{D_{THF}}$, the bulk quality of the single crystal integrity was significantly damaged since several micro-cracks always appeared at the surface of the crystals. As a result, the mosaicity of these single crystals was severely hampered but X-ray diffraction data collection was still possible to be conducted allowing getting access to a data set that can be used to proceed to the X-ray crystal structure resolution. Nevertheless, due to the low quality of the intrinsic mosaicity of these solvated single crystals, final agreement (R) factors were determinate with modest values (Table S1) and several ALERTs level B appear in the checkcif reports. Nevertheless, anisotropic displacement parameters associated to the atoms of these 1D-CPs are always satisfactory, unless specifically mentioned (*vide infra*) in the detailed description of each different X-ray crystal structure resolution. Indeed, some of the carbon atoms of the disordered phenyl rings had to be modelled with isotropic displacement parameters. This allows a primarily assignment of these modest R1 and *w*R2 factors of the derivative $\mathbf{D_{CH2Cl2}}$, $\mathbf{D_{EtOH}}$, $\mathbf{D_{CH3NO2}}$ or $\mathbf{D_{THF}}$ to the low mosaicity associated with the single crystals exposed to the vapochromic transition, and leads confidence to the treatment of the structural resolution of these derivatives whose metric data are fully consistent with those determined for $\mathbf{D_{dry}}$.

Concerning the X-ray crystal structure resolution of $\mathbf{D_{dry}}$, as indicated by an Alert Level B in the checkcif report, the “Structure Contains Solvent Accessible VOIDS”. Nevertheless, no residual electronic density can found in located in these voids. The protons of the aqua ligand were localized and were refined with isotropic displacement parameters. Table S1 gives the crystallographic data for the derivatives $\mathbf{D_{dry}}$.

Concerning the X-ray crystal structure resolution of $\mathbf{D_{CH2Cl2}}$, two included dichloromethane solvent molecules were found being highly disordered. A correct modelling of the disorder of these solvent molecules was not possible. We have therefore proceeded to a ‘squeeze’ treatment’[4] in order to remove the scattering contribution of these molecules which cannot be satisfactorily modelled. As a result, since these disordered molecules occupy a significant volume of the unit cell, several ALERTs level B appear in the checkcif report since " VERY LARGE Solvent Accessible VOIDs" are present in the structure resolution. In addition, one of the phenyl ring of one of the dppm ligands was found disordered over two neighboring positions whose relative occupancies were pondered. In the case of the orientation having the lowest ponderation in its occupancy, all the carbon atoms were refined with isotropic displacement parameters. Table S1 gives the crystallographic data for the derivative $\mathbf{D_{CH2Cl2}}$ after the ‘squeeze’ treatment. Table S2 give the crystallographic data for the derivative $\mathbf{D_{CH2Cl2}}$ before ‘squeeze’ treatment.

Concerning the X-ray crystal structure resolution of $\mathbf{D_{EtOH}}$, 1.5 included ethanol solvent molecules were found being highly disordered. A correct modelling of the disorder of these solvent molecules was not possible. We have therefore proceeded to a ‘squeeze’ treatment[4] in order to remove the scattering contribution of these molecules which cannot be satisfactorily modelled. As a result, since these disordered molecules occupy a significant volume of the unit cell, several ALERTs level A and level B appear in the checkcif report since "VERY LARGE Solvent Accessible VOIDs" are present in the structure resolution. In addition, one of the phenyl ring of one of the dppm ligands was found disordered over two neighboring positions whose relative occupancies were pondered. Some of the carbon atoms of the phenyl rings of the dppm ligands were refined with isotropic displacement parameters, which induced apparition of several ALERTs level B the checkcif report. Finally, in the case of the X-ray crystal structure resolution of $\mathbf{D_{EtOH}}$, the protons of the aqua ligand could be localized and were refined with isotropic displacement parameters. Table S1 gives the crystallographic data for the derivative $\mathbf{D_{EtOH}}$ after the ‘squeeze’ treatment. Table S2 give the crystallographic data for the derivative $\mathbf{D_{EtOH}}$ before ‘squeeze’ treatment.

Concerning the X-ray crystal structure resolution of $\mathbf{D_{CH3NO2}}$, one included nitromethane solvent molecules was found being highly disordered. A correct modelling of the disorder of this solvent molecule was not possible. We have therefore proceeded to a ‘squeeze’ treatment[4] in order to remove the scattering contribution of this molecules which cannot be satisfactorily modelled. As a result, since this disordered molecule occupy a significant volume of the unit cell, several ALERTs level A and level B appear in the checkcif report since " VERY LARGE Solvent Accessible VOIDs" are present in the structure resolution. In addition, one of the phenyl ring of one of the dppm ligands was found disordered over two neighboring positions whose relatives occupancies were ponderated. Finally, in the case of the X-ray crystal structure resolution of $\mathbf{D_{CH3NO2}}$, the protons of the aqua ligand could be localized and were refined with isotropic displacement parameters. Table S1 gives the crystallographic data for the derivative $\mathbf{D_{CH3NO2}}$ after the ‘squeeze’ treatment. Table S2 give the crystallographic data for the derivative $\mathbf{D_{CH3NO2}}$ before ‘squeeze’ treatment.

Concerning the X-ray crystal structure resolution of $\mathbf{D_{THF}}$, one included THF solvent molecule was found being highly disordered over two neighboring positions whose relative occupancies were first pondered. Nevertheless, an acceptable modelling of the disorder of this solvent molecule was not possible. We have therefore proceeded to a ‘squeeze’ treatment[4] in order to remove the scattering contribution of this molecule which cannot be satisfactorily modelled. As a result, since this disordered molecule occupy a significant volume of the unit cell, several ALERTs level A and level B appear in the checkcif report since " VERY LARGE Solvent Accessible VOIDs" are present in the structure resolution. In addition, one of the phenyl ring of one of the dppm ligands was found disordered over two neighboring positions whose relative occupancies were pondered. Finally, in the case of the X-ray crystal structure resolution of $\mathbf{D_{THF}}$, the protons of the aqua ligand were localized and were refined with isotropic displacement parameters. Table S1 gives the crystallographic data for the derivative $\mathbf{D_{THF}}$ after the ‘squeeze’ treatment. Table S2 give the crystallographic data for the derivative $\mathbf{D_{THF}}$ before ‘squeeze’ treatment.

Atomic scattering factors for all atoms were taken from International Tables for X-ray Crystallography.[5] CCDC reference numbers 2005250, 2005249, 2005253, 2005252 and 2005251 contain the supplementary crystallographic data for the reference measurements of the X-ray crystal structures of the derivatives $\mathbf{D_{dry}}$, $\mathbf{D_{CH2Cl2}}$, $\mathbf{D_{EtOH}}$, $\mathbf{D_{CH3NO2}}$ or $\mathbf{D_{THF}}$ respectively. These data can be obtained free of charge from the Cambridge Crystallographic Data Centre.

**Table S1.** Crystal data and structure refinement for derivatives $\mathbf{D}_{\mathbf{dry}}$, $\mathbf{D}_{\mathbf{CH2Cl2}}$, $\mathbf{D}_{\mathbf{EtOH}}$, $\mathbf{D}_{\mathbf{CH3NO2}}$ or $\mathbf{D}_{\mathbf{THF}}$ after the ‘squeeze’ treatment

| | $\mathbf{D}_{\mathbf{dry}}$ | $\mathbf{D}_{\mathbf{CH2Cl2}}$ | $\mathbf{D}_{\mathbf{EtOH}}$ |
|---|---|---|---|
| Molecular formula | $C_{58}H_{50}Cu_2F_{12}N_2OP_6$ | $C_{58}H_{50}Cu_2F_{12}N_2OP_6$ | $C_{58}H_{50}Cu_2F_{12}N_2OP_6$ |
| CCDC number | 2005250 | 2005249 | 2005253 |
| Molecular weight | 1331.90 | 1331.90 | 1331.90 |
| $a$(Å) | 13.2578(6) | 13.972(2) | 13.843(2) |
| $b$ (Å) | 22.1788(9) | 22.320(3) | 22.710(3) |
| $c$ (Å) | 20.6890(12) | 20.342(3) | 20.222(3) |
| $\alpha$ (°) | 90 | 90 | 90 |
| $\beta$ (°) | 91.1534(20) | 92.108(6) | 91.308(5) |
| $\gamma$ (°) | 90 | 90 | 90 |
| $V$ (Å$^3$) | 6082.2(5) | 6339.5(16) | 6355.6(16) |
| $Z$ | 4 | 4 | 4 |
| $Dc$ (g cm$^{-3}$) | 1.454 | 1.396 | 1.392 |
| Crystal system | Monoclinic | Monoclinic | Monoclinic |
| Space group | P21/c | P21/c | P21/c |
| Temperature (K) | 150(2) | 150(2) | 150(2) |
| Wavelength Mo-$K\alpha$ (Å) | 0.71069 | 0.71073 | 0.71073 |
| Crystal size (mm) | 0.4 * 0.23 * 0.1 | 0.26 * 0.21 * 0.11 | 0.18 * 0.15 * 0.11 |
| $\mu$ (mm$^{-1}$) | 0.934 | 0.896 | 0.894 |
| $F$(000) | 2704 | 2704 | 2704 |
| $\theta$ limit (°) | 1.35 –26.40 | 2.08 –27.71 | 2.21 –27.60 |
| Index ranges $hkl$ | $-11 \leq h \leq 16$,<br>$-27 \leq k \leq 27$,<br>$-25 \leq l \leq 25$ | $-17 \leq h \leq 18$,<br>$-29 \leq k \leq 29$,<br>$-25 \leq l \leq 26$ | $-17 \leq h \leq 17$,<br>$-26 \leq k \leq 29$,<br>$-24 \leq l \leq 26$ |
| Reflections collected | 25533 | 109973 | 46284 |
| Independant reflections | 12378 | 14522 | 14390 |
| Reflections [$I$>2$\sigma$($I$)] | 7932 | 10023 | 9418 |
| Data/restraints/parameters | 12378/ 0 / 737 | 14522/ 0 / 732 | 14390/ 0 / 741 |
| Goodness-of-fit on $F^2$ | 1.027 | 1.043 | 1.055 |
| Final $R$ indices [$I$>2$\sigma$($I$)] | R1= 0.0614<br>wR2= 0.1428 | R1= 0.1560<br>wR2= 0.3695 | R1= 0.1134<br>wR2= 0.2232 |
| $R$ indices (all data) | R1= 0.1042<br>wR2= 0.1733 | R1= 0.1908<br>wR2= 0.3895 | R1= 0.1602<br>wR2= 0.2479 |
| Largest diff peak and hole (e Å$^{-3}$) | 1.004 and -0.755 | 2.392 and -1.060 | 2.055 and -1.012 |

|  | **D$_{CH3NO2}$** | **D$_{THF}$** |
|---|---|---|
| Molecular formula | $C_{58}H_{50}Cu_2F_{12}N_2OP_6$ | $C_{58}H_{50}Cu_2F_{12}N_2OP_6$ |
| CCDC number | 2005252 | 2005251 |
| Molecular weight | 1331.90 | 1331.90 |
| $a$(Å) | 13.7187(9) | 13.983(2) |
| $b$ (Å) | 22.5661(13) | 22.598(3) |
| $c$ (Å) | 20.3718(14) | 20.222(3) |
| $\alpha$ (°) | 90 | 90 |
| $\beta$ (°) | 91.618(3) | 91.830(5) |
| $\gamma$ (°) | 90 | 90 |
| $V$ (Å$^3$) | 6304.1(7) | 6386.7(16) |
| $Z$ | 4 | 4 |
| $D$c (g cm$^{-3}$) | 1.403 | 1.385 |
| Crystal system | Monoclinic | Monoclinic |
| Space group | P21/c | P21/c |
| Temperature (K) | 150(2) | 150(2) |
| Wavelength Mo-$K\alpha$ (Å) | 0.71073 | 0.71069 |
| Crystal size (mm) | 0.19 * 0.16 * 0.12 | 0.25 * 0.17 * 0.11 |
| $\mu$ (mm$^{-1}$) | 0.901 | 0.890 |
| $F$(000) | 2704 | 2704 |
| $\theta$ limit (°) | 2.19 –27.55 | 2.21 –27.63 |
| Index ranges *hkl* | $-17 \leq h \leq 17$,<br>$-27 \leq k \leq 29$,<br>$-26 \leq l \leq 24$ | $-18 \leq h \leq 18$,<br>$-25 \leq k \leq 29$,<br>$-26 \leq l \leq 26$ |
| Reflections collected | 50324 | 73293 |
| Independant reflections | 14198 | 14779 |
| Reflections [$I>2\sigma(I)$] | 9561 | 8251 |
| Data/restraints/parameters | 14198/ 0 / 752 | 14779/ 0 / 769 |
| Goodness-of-fit on $F^2$ | 1.079 | 1.089 |
| Final $R$ indices [$I>2\sigma(I)$] | R1= 0.1230<br>wR2= 0.2434 | R1= 0.1092<br>wR2= 0.2675 |
| $R$ indices (all data) | R1= 0.1632<br>wR2= 0.2614 | R1= 0.1683<br>wR2= 0.3000 |
| Largest diff peak and hole (e Å$^{-3}$) | 2.181 and -1.327 | 1.397 and -0.953 |

**Table S2.** Crystal data and structure refinement for derivatives $\mathbf{D_{CH2Cl2}}$, $\mathbf{D_{EtOH}}$, $\mathbf{D_{CH3NO2}}$ or $\mathbf{D_{THF}}$ before the ‘squeeze’ treatment

|  | $\mathbf{D_{CH2Cl2}}$. **2 $CH_2Cl_2$** | $\mathbf{D_{EtOH}}$. **1.5ETOH** | $\mathbf{D_{CH3NO2}}$. **$CH_3NO_2$** | $\mathbf{D_{THF}}$ **. THF** |
|---|---|---|---|---|
| Molecular formula | $C_{60}H_{48}Cl_4Cu_2F_{12}N_2OP_6$ | $C_{61}H_{59}Cu_2F_{12}N_2O_{2.5}P_6$ | $C_{59}H_{53}Cu_2F_{12}N_3O_3P_6$ | $C_{62}H_{56}Cu_2F_{12}N_2O_2P_6$ |
| Molecular weight | 1495.70 | 1401.00 | 1392.94 | 1401.99 |
| $a$(Å) | 13.972(2) | 13.843(2) | 13.7187(9) | 13.983(2) |
| $b$ (Å) | 22.320(3) | 22.710(3) | 22.5661(13) | 22.598(3) |
| $c$ (Å) | 20.342(3) | 20.222(3) | 20.3718(14) | 20.222(3) |
| $\alpha$ (°) | 90 | 90 | 90 | 90 |
| $\beta$ (°) | 92.108(6) | 91.308(5) | 91.618(3) | 91.830(5) |
| $\gamma$ (°) | 90 | 90 | 90 | 90 |
| $V$ (Å$^3$) | 6339.4(16) | 6355.6(15) | 6304.1(7) | 6387(3) |
| $Z$ | 4 | 4 | 4 | 4 |
| $D$c (g cm$^{-3}$) | 1.567 | 1.464 | 1.468 | 1.458 |
| Crystal system | Monoclinic | Monoclinic | Monoclinic | Monoclinic |
| Space group | P21/c | P21/c | P21/c | P21/c |
| Temperature (K) | 293(2) | 293(2) | 293(2) | 293(2) |
| Wavelength Mo-$K\alpha$ (Å) | 0.71073 | 0.71073 | 0.71073 | 0.71069 |
| Crystal size (mm) | 0.26 * 0.21 * 0.11 | 0.18 * 0.15 * 0.11 | 0.19 * 0.16 * 0.12 | 0.25 * 0.17 * 0.11 |
| $\mu$ (mm$^{-1}$) | 1.069 | 0.900 | 0.908 | 0.895 |
| $F$(000) | 3016 | 2860 | 2832 | 2856 |
| $\theta$ limit (°) | 2.08 –27.71 | 2.21 –27.60 | 2.19 –27.55 | 2.21 –27.63 |
| Index ranges $hkl$ | $-17 \leq h \leq 18$, | $-17 \leq h \leq 17$, | $-17 \leq h \leq 17$, | $-18 \leq h \leq 18$, |
|  | $-29 \leq k \leq 29$, | $-26 \leq k \leq 29$, | $-27 \leq k \leq 29$, | $-25 \leq k \leq 29$, |
|  | $-25 \leq l \leq 26$ | $-24 \leq l \leq 26$ | $-26 \leq l \leq 24$ | $-26 \leq l \leq 26$ |
| Reflections collected | 109973 | 46284 | 50324 | 73293 |
| Independant reflections | 14522 | 14390 | 14198 | 14779 |
| Reflections [$I$>2$\sigma$($I$)] | 9975 | 9532 | 9688 | 8137 |
| Data/restraints/parameters | 14522/ 0 / 831 | 14390/ 0 / 817 | 14198/ 6 / 798 | 14779/ 20 / 853 |
| Goodness-of-fit on $F^2$ | 1.112 | 1.194 | 1.203 | 1.106 |
| Final $R$ indices [$I$>2$\sigma$($I$)] | R1= 0.1775 | R1= 0.1172 | R1= 0.1357 | R1= 0.1212 |
|  | wR2= 0.3649 | wR2= 0.2225 | wR2= 0.2733 | wR2= 0.2697 |
| $R$ indices (all data) | R1= 0.2239 | R1= 0.1784 | R1= 0.1871 | R1= 0.2148 |
|  | wR2= 0.3918 | wR2= 0.2593 | wR2= 0.3004 | wR2= 0.3365 |
| Largest diff peak and hole (e Å$^{-3}$) | 2.045 and -1.170 | 1.900 and -0.870 | 1.622 and -1.301 | 1.602 and -0.971 |

**Table S3**. Intermetallic distances [Å] and angles [°] for the $\mathbf{D_{dry}}$, $\mathbf{D_{CH2Cl2}}$, $\mathbf{D_{EtOH}}$, $\mathbf{D_{CH3NO2}}$ or $\mathbf{D_{THF}}$

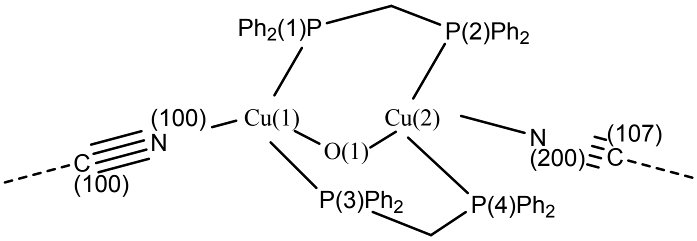

| | $\mathbf{D_{dry}}$ | $\mathbf{D_{CH2Cl2}}$ | $\mathbf{D_{EtOH}}$ | $\mathbf{D_{CH3NO2}}$ | $\mathbf{D_{THF}}$ |
|---|---|---|---|---|---|
| **Cu(1)-Cu(2)** | 3.1300(9) | 3.132(2) | 3.179(1) | 3.1799(9) | 3.157(1) |
| **Cu(1)-O(1)** | 2.222(3) | 2.222(7) | 2.225(5) | 2.216(4) | 2.207(6) |
| **Cu(2)-O(1)** | 2.339(4) | 2.359(7) | 2.393(5) | 2.353(4) | 2.362(6) |
| **Cu(1)-N(100)** | 2.022(4) | 2.014(9) | 2.014(6) | 2.025(5) | 2.019(7) |
| **Cu(2)-N(200)** | 2.009(4) | 2.006(9) | 2.026(6) | 2.018(5) | 2.013(7) |
| **Cu(1)-P(1)** | 2.2287(13) | 2.206(3) | 2.284(2) | 2.2589(17) | 2.218(2) |
| **Cu(1)-P(3)** | 2.2494(15) | 2.246(3) | 2.2594(19) | 2.2221(15) | 2.243(2) |
| **Cu(2)-P(2)** | 2.2634(13) | 2.237(3) | 2.252(2) | 2.2813(18) | 2.241(2) |
| **Cu(2)-P(4)** | 2.2735(16) | 2.270(3) | 2.2262(18) | 2.2596(16) | 2.264(3) |
| **Cu(1)-O(1)-Cu(2)** | 86.63(11) | 86.2(2) | 86.94(19) | 88.15(14) | 87.3(2) |
| **Cu(1)-N(100)-C(100)** | 154.6(4) | 157.6(10) | 160.1(6) | 157.8(5) | 157.0(7) |
| **Cu(2)-N(200)-C(107)** | 158.7(4) | 161.5(9) | 157.9(7) | 160.7(5) | 159.4(7) |

**Table S4.** Unit cell parameters for derivatives $\mathbf{D_{Dry}}$ and $\mathbf{D_{CH2Cl2}}$ at 150 K, 200 K and 250 K.

| | $\mathbf{D_{Dry}}$ **150K** | $\mathbf{D_{Dry}}$ **200K** | $\mathbf{D_{Dry}}$ **250K** | $\mathbf{D_{CH2Cl2}}$ **150K** | $\mathbf{D_{CH2Cl2}}$ **200K** | $\mathbf{D_{CH2Cl2}}$ **250K** |
|---|---|---|---|---|---|---|
| $a$(Å) | 13.2578(6) | 13.29(2) | 13.36(3) | 13.972(2) | 13.99(2) | 14.03(3) |
| $b$ (Å) | 22.1788(9) | 22.25(3) | 22.31(3) | 22.320(3) | 22.42(2) | 22.55(4) |
| $c$ (Å) | 20.6890(12) | 20.62(2) | 20.66(3) | 20.342(3) | 20.36(2) | 20.37(3) |
| $\alpha$ (°) | 90 | 90 | 90 | 90 | 90 | 90 |
| $\beta$ (°) | 91.1534(20) | 90.55(4) | 90.91(5) | 92.108(6) | 92.12(6) | 92.41(6) |
| $\gamma$ (°) | 90 | 90 | 90 | 90 | 90 | 90 |

**Fig. S2.** ORTEP views of the molecular structure of the repetition unit of the 1D-CPs **D$_{\mathbf{dry}}$**. Hydrogen atoms and hexafluorophosphate counter-anions have been omitted for clarity.

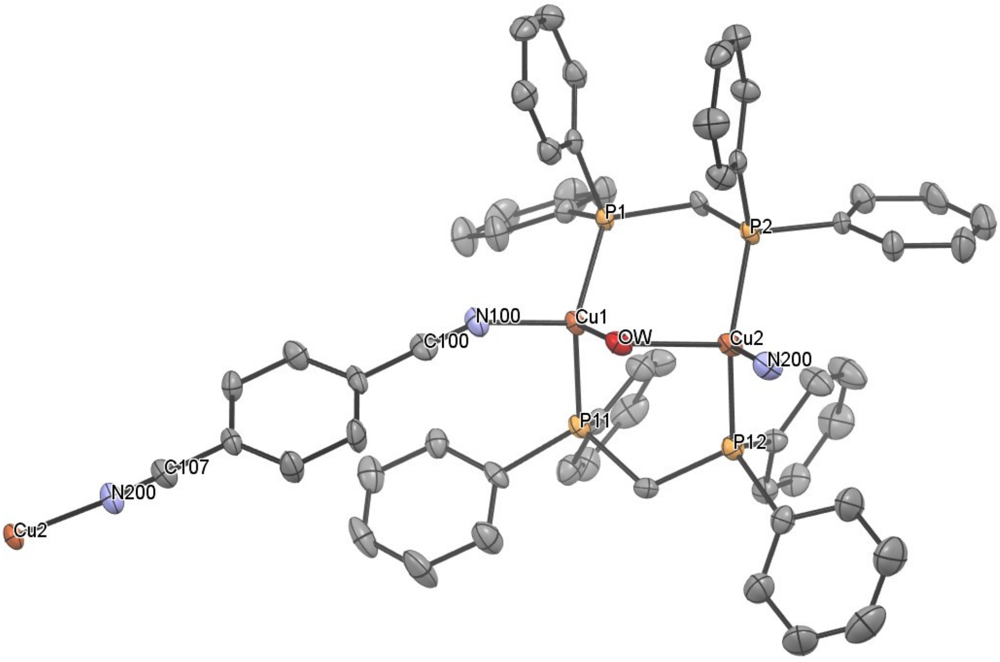

**Fig. S3.** ORTEP views of the molecular structure of the repetition unit of the 1D-CPs (a) $\mathbf{D_{CH2Cl2}}$, after the squeeze treatment: hydrogen atoms and hexafluorophosphate counter-anions have been omitted for clarity; the phenyl ring that was modelled with two relative orientations is represented in grey for the atoms of the phenyl ring having the highest ponderation and in white for the phenyl ring having the lowest ponderation (for which carbon atoms could be refined only with isotropic displacement parameters; (b) $\mathbf{D_{CH2Cl}}$ **.** $\mathbf{2CH_2Cl_2}$ before the squeeze treatment: hydrogen atoms have been omitted for clarity; the phenyl rings that were modelled with two relative orientations are represented in grey for the atoms of the phenyl ring having the highest ponderation and in white for the phenyl ring having the lowest ponderation; the two included very disordered $CH_2Cl_2$ solvent molecules are shown in the stick and ball graphical mode with only one orientation for one of them and with the two orientations of the second one shown with pale colors for the orientations having the lower ponderation in its relative occupancy.

a)

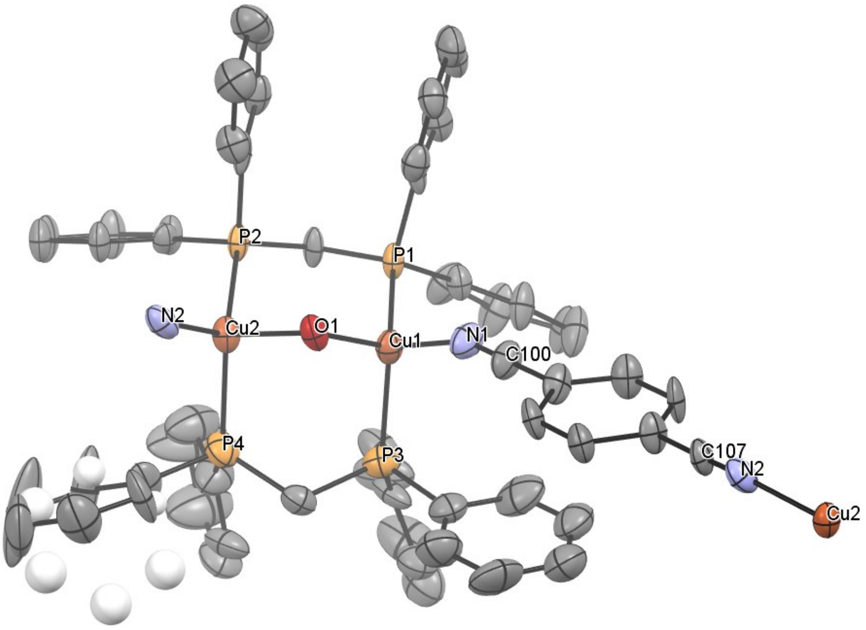

b)

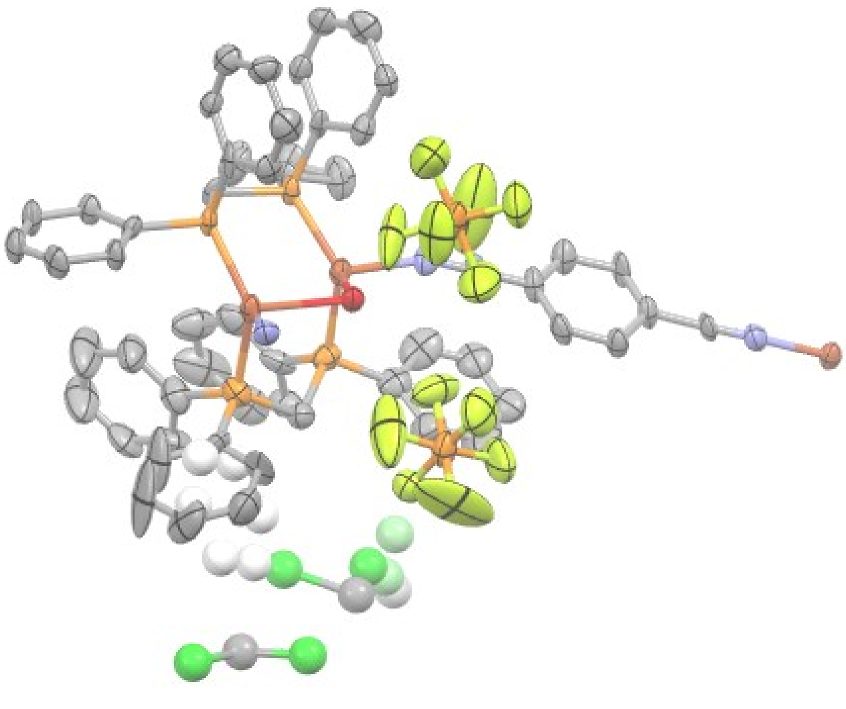

**Fig. S4.** ORTEP views of the molecular structure of the repetition unit of the 1D-CPs (a) $\mathbf{D_{EtOH}}$, after the squeeze treatment: hydrogen atoms and hexafluorophosphate counter-anions have been omitted for clarity; the phenyl ring that was modelled with two relative orientations is represented in grey for the atoms of the phenyl ring having the highest ponderation and in white for the phenyl ring having the lowest ponderation; (b) $\mathbf{D_{EtOH}}$ **. 1.5 EtOH** before the squeeze treatment: hydrogen atoms have been omitted for clarity; the phenyl ring that was modelled with two relative orientations is represented in grey for the atoms of the phenyl ring having the highest ponderation and in white for the phenyl ring having the lowest ponderation; the 1.5 included disordered EtOH solvent molecules are shown in the stick and ball graphical mode with pale colors for the molecule having the lower occupancy.

a)

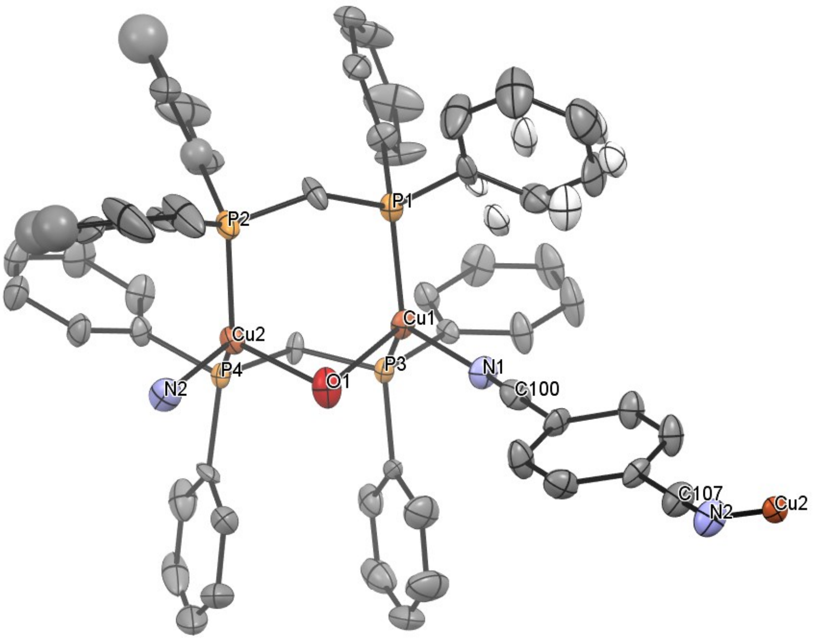

b)

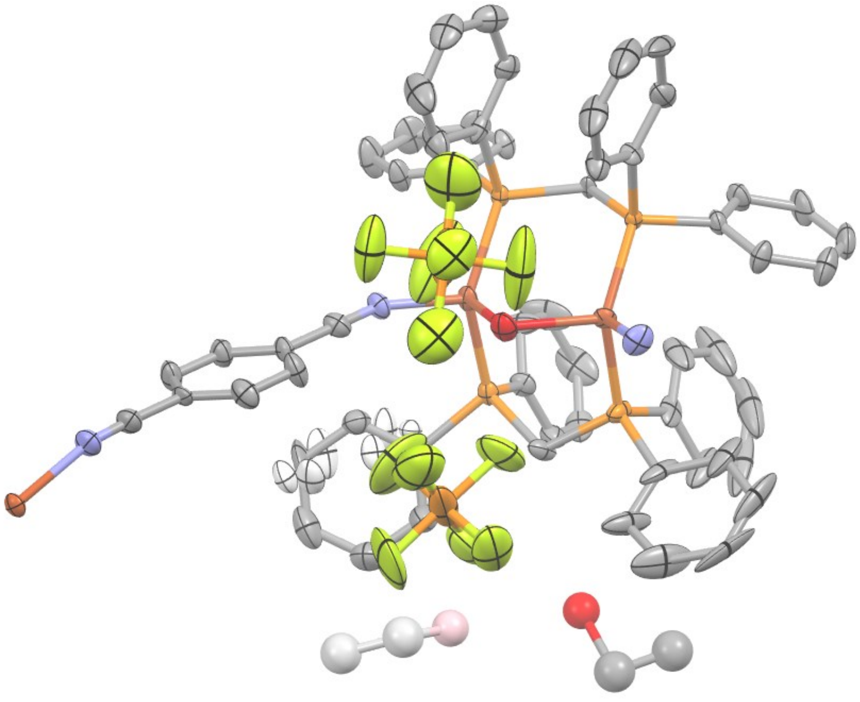

**Fig. S5.** ORTEP views of the molecular structure of the repetition unit of the 1D-CPs (a) $\mathbf{D_{CH3NO2}}$, after the squeeze treatment: hydrogen atoms and hexafluorophosphate counter-anions have been omitted for clarity; the phenyl ring that was modelled with two relative orientations is represented in grey for the atoms of the phenyl ring having the highest ponderation and in white for the phenyl ring having the lowest ponderation; (b) $\mathbf{D_{CH3NO2} \cdot CH_3NO_2}$ before the squeeze treatment: hydrogen atoms have been omitted for clarity; the phenyl ring that was modelled with two relative orientations is represented in grey for the atoms of the phenyl ring having the highest ponderation and in white for the phenyl ring having the lowest ponderation; the included disordered $CH_3NO_2$ solvent molecule is shown in the stick and ball graphical mode.

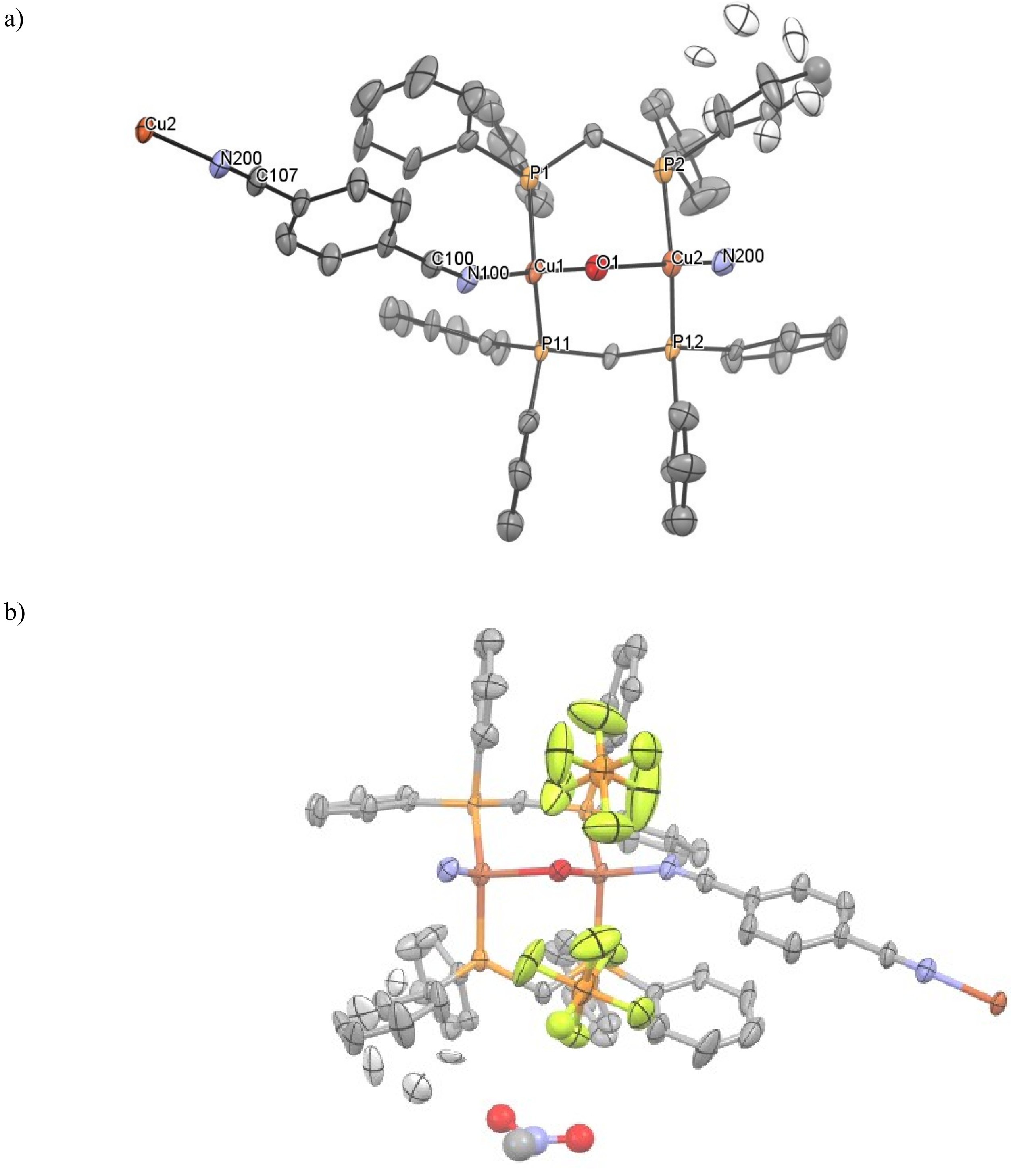

**Fig. S6.** ORTEP views of the molecular structure of the repetition unit of the 1D-CPs (a) $\mathbf{D_{THF}}$, after the squeeze treatment: hydrogen atoms and hexafluorophosphate counter-anions have been omitted for clarity; the phenyl ring that was modelled with two relative orientations is represented in grey for the atoms of the phenyl ring having the highest ponderation and in white for the phenyl ring having the lowest ponderation; (b) $\mathbf{D_{THF}}$ **. THF** before the squeeze treatment: hydrogen atoms have been omitted for clarity; the phenyl ring that was modelled with two relative orientations is represented in grey for the atoms of the phenyl ring having the highest ponderation and in white for the phenyl ring having the lowest ponderation; only one orientation of the included disordered THF solvent molecule is shown in the stick and ball graphical mode.

a)

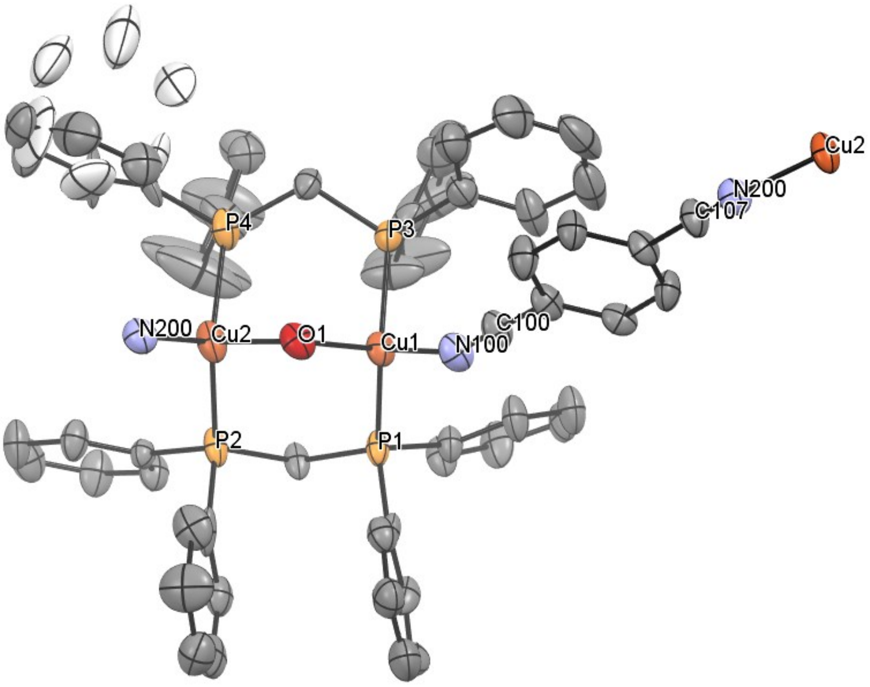

b)

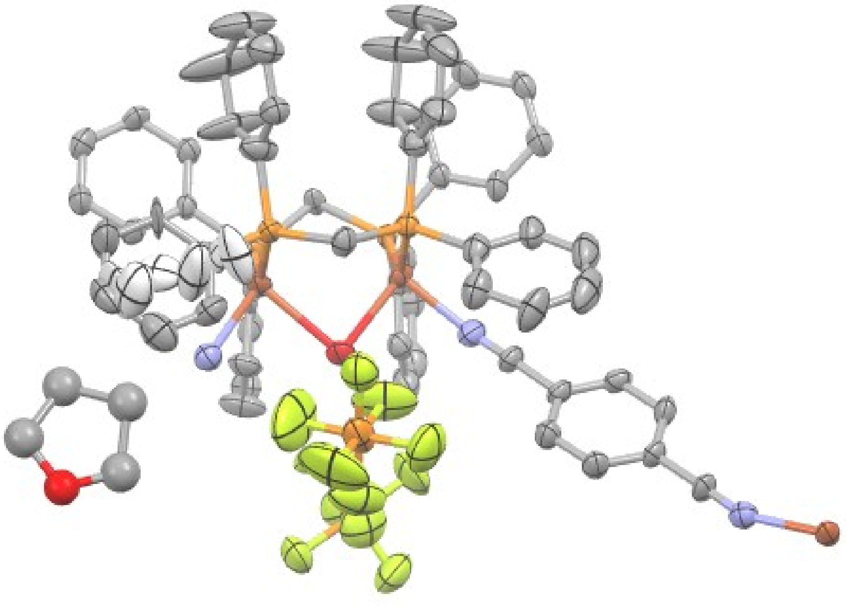

## III. Photophysical study

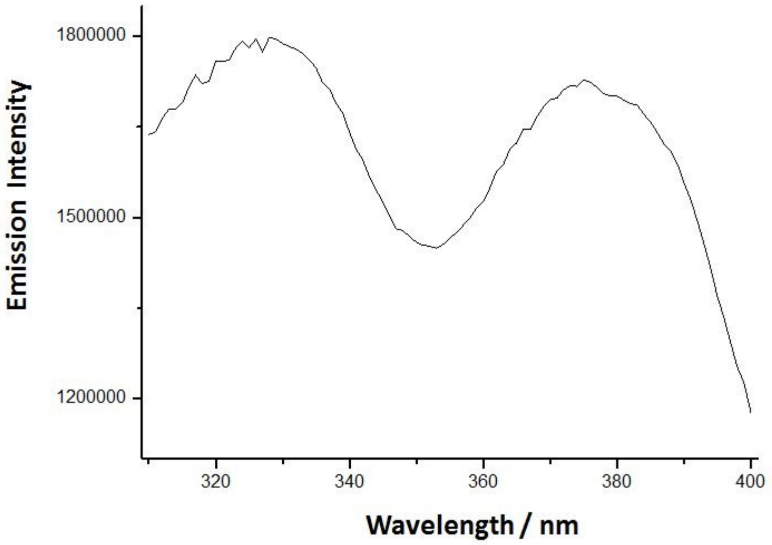

**Fig. S7.** RT solid state excitation spectrum of **Ddry** at 298 K

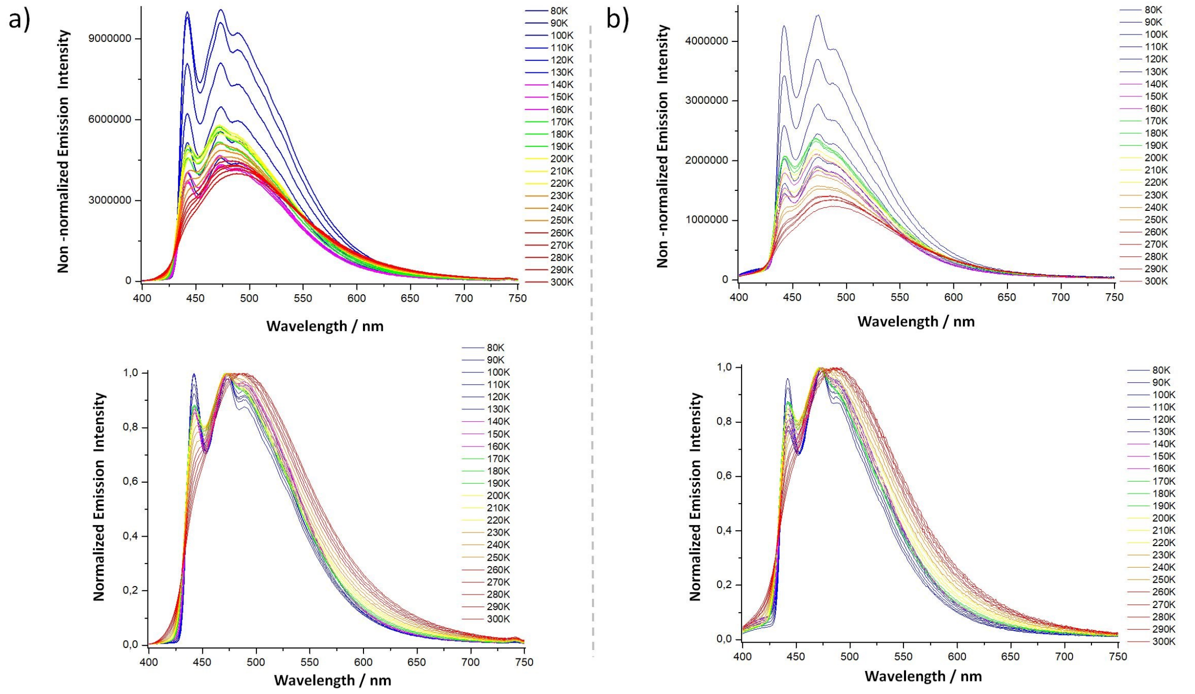

**Fig. S8**. Temperature-dependent non-normalized (top, arbitrary units) and normalized (bottom) solid state emission spectra of **Ddry** with a) $\lambda_{exc} = 370$ nm and b) $\lambda_{exc} = 330$ nm ; from 80 K to 298 K.

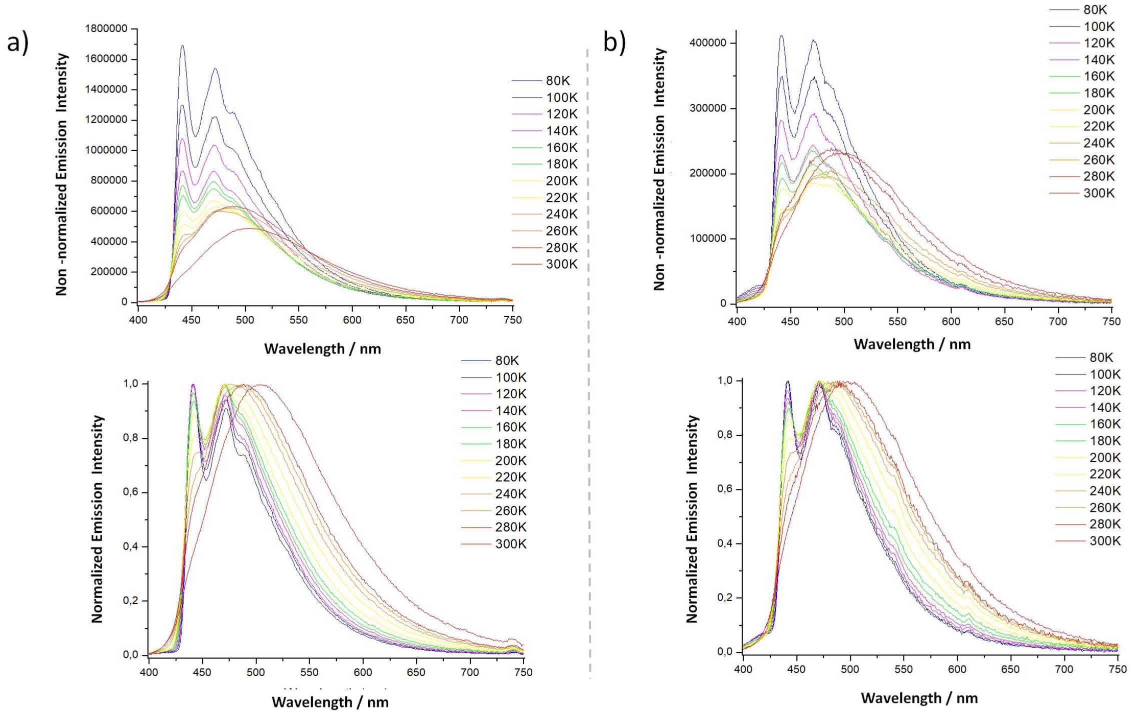

**Fig. S9**. Temperature-dependent non-normalized (top, arbitrary units) and normalized (bottom) solid state emission spectra of $\mathbf{D}_{\mathbf{CH2Cl2}}$ with a) $\lambda_{exc}$ = 370 nm and b) $\lambda_{exc}$ = 330 nm ; from 80 K to 298 K.

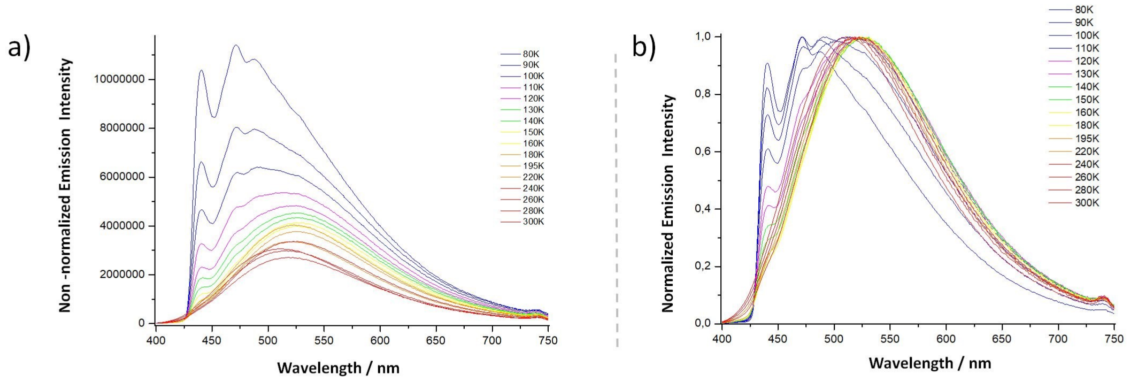

**Fig. S10**. a) Temperature-dependent non-normalized (arbitrary units) and b) normalized solid state emission spectra of $\mathbf{D}_{\mathbf{EtOH}}$ with $\lambda_{exc}$ = 370 nm; from 80 K to 298 K.

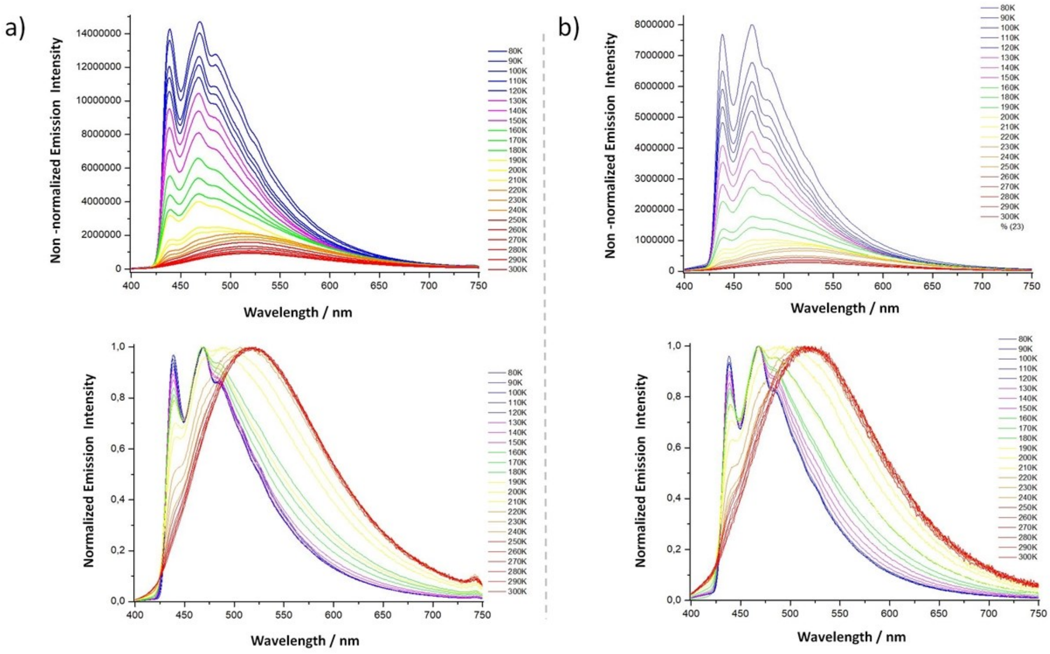

**Fig. S11**. Temperature-dependent non-normalized (top, arbitrary units) and normalized (bottom) solid state emission spectra of $\mathbf{D_{CH3NO2}}$ with a) $\lambda_{exc}$ = 370 nm and b) $\lambda_{exc}$ = 330 nm ; from 80 K to 298 K.

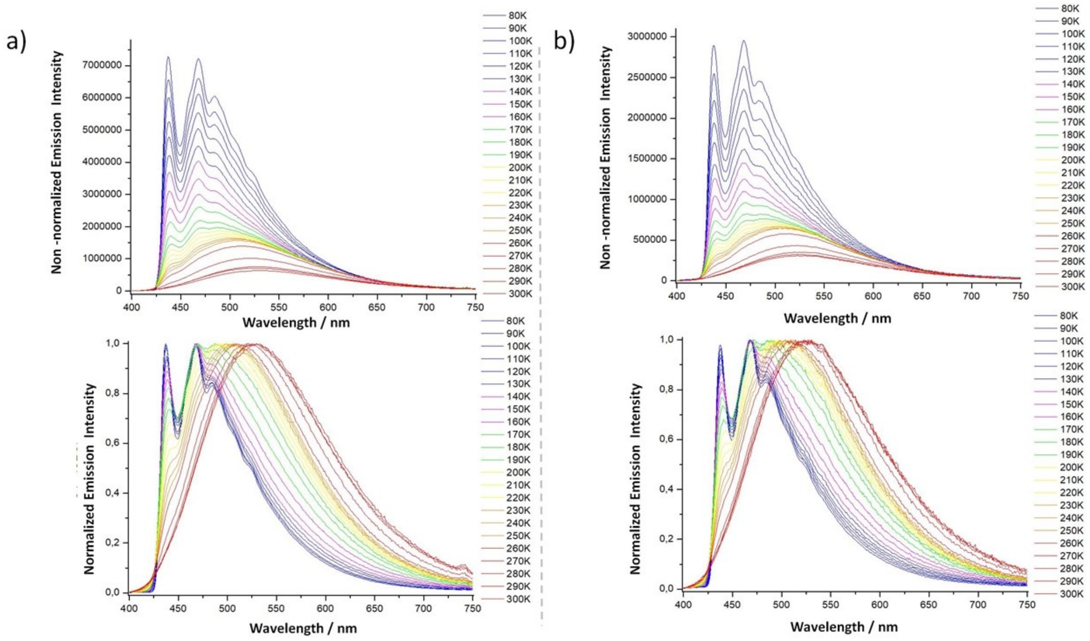

**Fig. S12**. Temperature-dependent non-normalized (top, arbitrary units) and normalized (bottom) solid state emission spectra of $\mathbf{D_{THF}}$ with a) $\lambda_{exc}$ = 370 nm and b) $\lambda_{exc}$ = 330 nm ; from 80 K to 298 K.

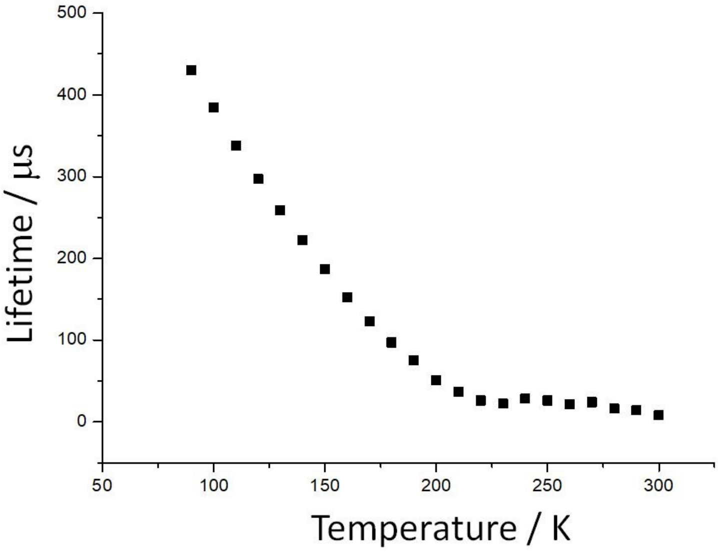

**Fig. S13**. Plot of emission decay lifetime against temperature (80 K to 300 K) of $\mathbf{D_{CH3NO2}}$ with $\lambda_{exc}$ = 370 nm.

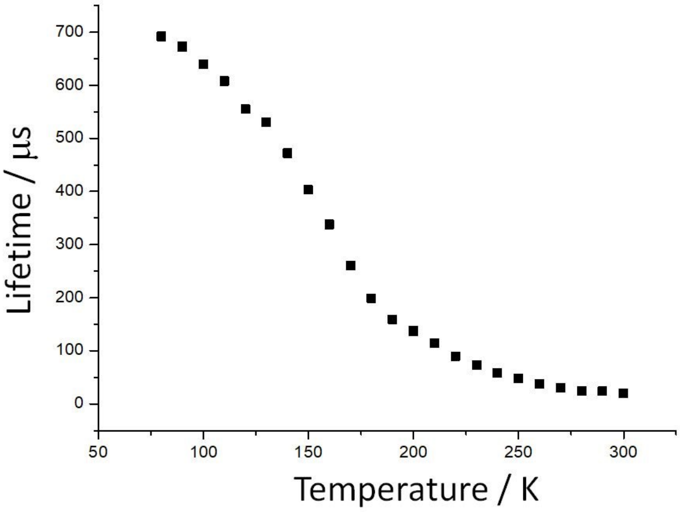

**Fig. S14**. Plot of emission decay lifetime against temperature (80 K to 300 K) of $\mathbf{D_{THF}}$ with $\lambda_{exc}$ = 370 nm.

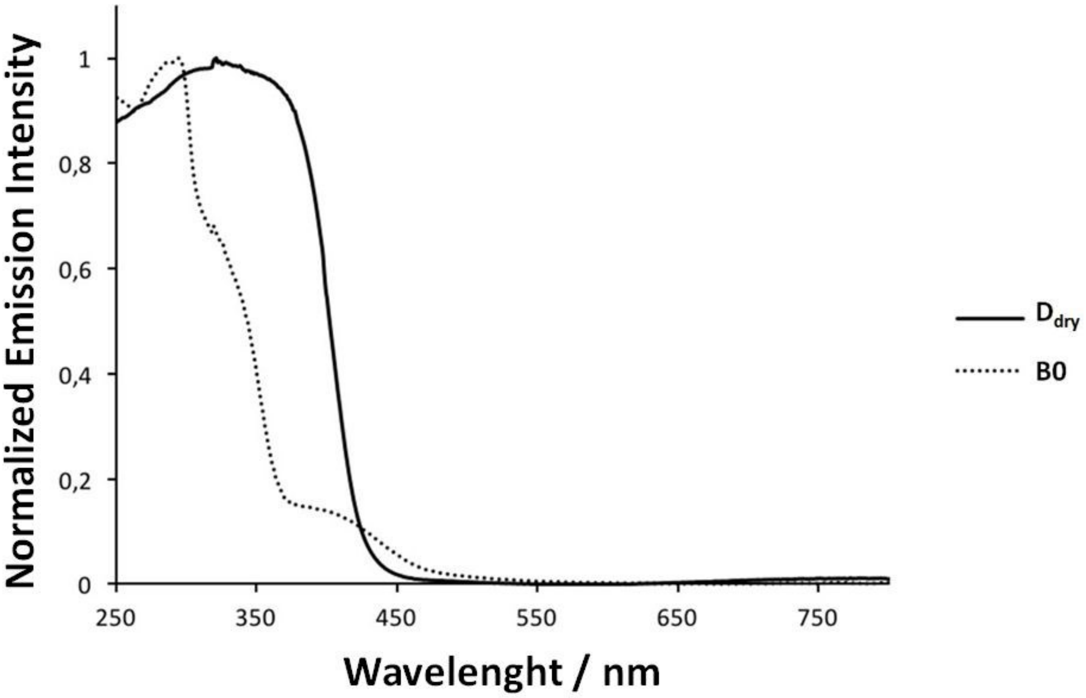

**Fig. S15**. Solid state UV-Vis absorption spectrum of **$D_{dry}$** and ligand **B0** at room temperature.

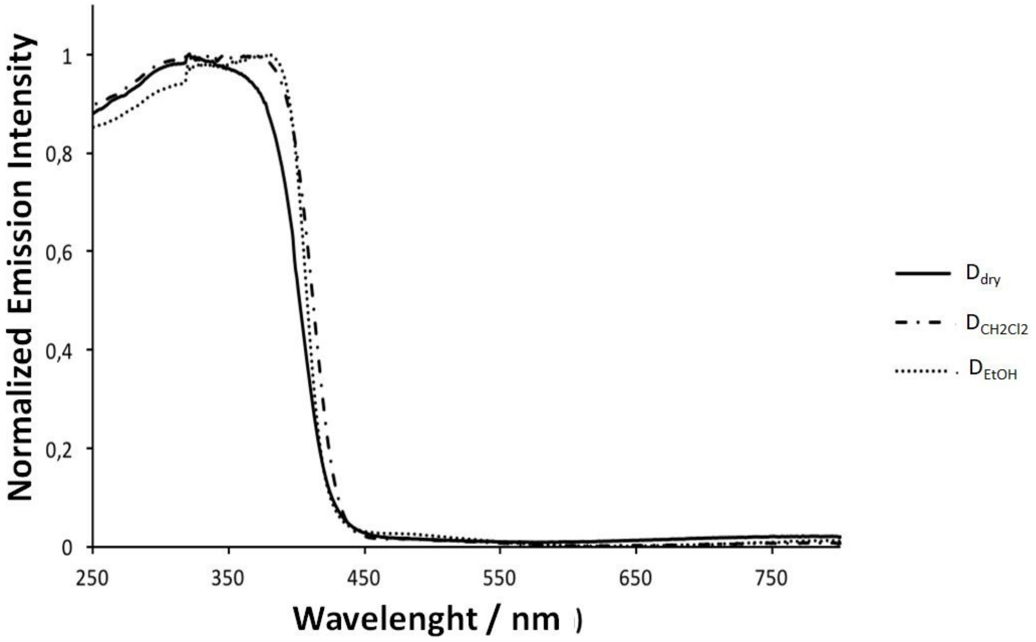

**Fig. S16**. Solid state UV-Vis absorption spectrum of **$D_{dry}$, $D_{CH2Cl2}$ and $D_{EtOH}$** at room temperature.

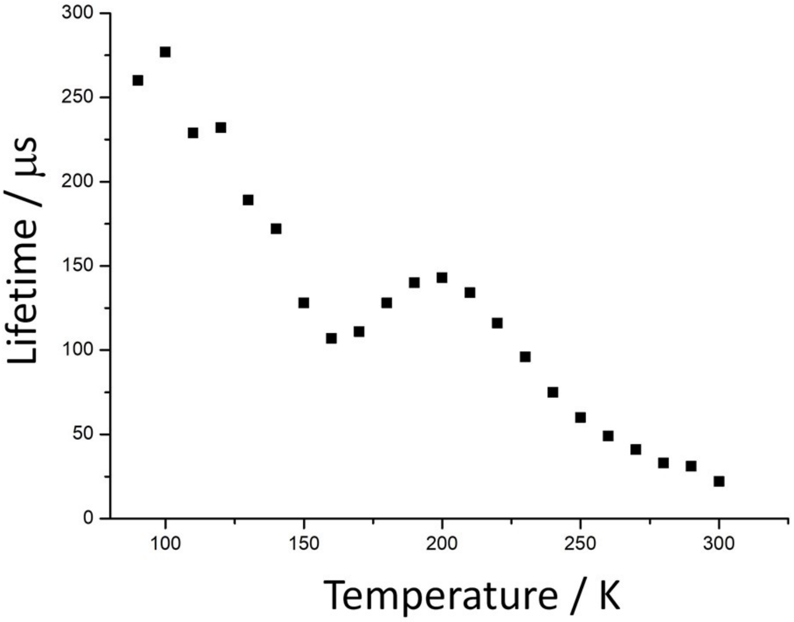

**Fig. S17**. Plot of emission decay lifetime against temperature of $\mathbf{D_{dry}}$ with $\lambda_{exc}$ = 370 nm performed on a second and independent batch of derivative $\mathbf{D_{dry}}$.

## IV. Computational details

DFT calculations were carried out using the Gaussian 09 program.[6] A molecular fragment of the polymer, $[Cu_2(\mu_2\text{-dppm})_2(1,4\text{-dicyanobenzene})_2]$ was extracted from the $\mathbf{D_{Dry}}$ X-Ray structure (see Scheme S1). All calculations were performed using PBE0[7] functional and SVP[8] atomic basis set. Tight criterion of energy convergence were applied to ensure high quality of calculations ($10^{-10}$ u.a.). Only the carbon and hydrogen atomic positions were optimized for the ground state configuration ($S_0$) to maintain mostly the solid-state configuration. The vertical electronic excitation energies of the first vertical singlet and triplet excited states were calculated by time-dependant DFT protocol. A complete study would imply geometry optimizations of the excited states that could be comparable to the emission experimental data. This would necessitate to take into account the polymer and crystal reorganisation / relaxations that constrain the molecular fragment which is not possible at this molecular level of simulation.

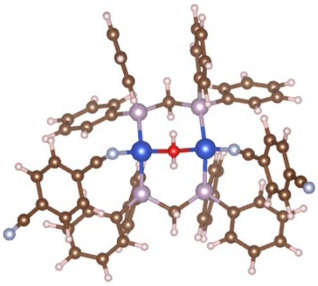

**Scheme S1**

**Table S4.** Calculated vertical electronic excited state energies of [$Cu_2(\mu^2$-dppm$)_2$(1,4-dicyanobenzene$)_2$] and associated oscillator strength (zero for the triplet states in the absence of spin-orbit coupling consideration).

| Singlet Excited States | Excitation Energy (eV) | λ (nm) | Oscillator Strength | Triplet Excited States | Excitation Energy (eV) |
|---|---|---|---|---|---|
| $S_1$ | 3.526 | 352 | 0.004 | $T_1$ | 2.902 |
| $S_2$ | 3.564 | 348 | 0.014 | $T_2$ | 2.904 |
| $S_3$ | 3.625 | 342 | 0.039 | $T_3$ | 3.425 |
| $S_4$ | 3.754 | 330 | 0.044 | $T_4$ | 3.445 |
| $S_5$ | 3.906 | 328 | 0.002 | $T_5$ | 3.457 |
| $S_6$ | 4.070 | 317 | 0.003 | $T_6$ | 3.468 |
| $S_7$ | 3.783 | 305 | 0.001 | $T_7$ | 3.469 |
| $S_8$ | 4.131 | 300 | 0.003 | $T_8$ | 3.478 |

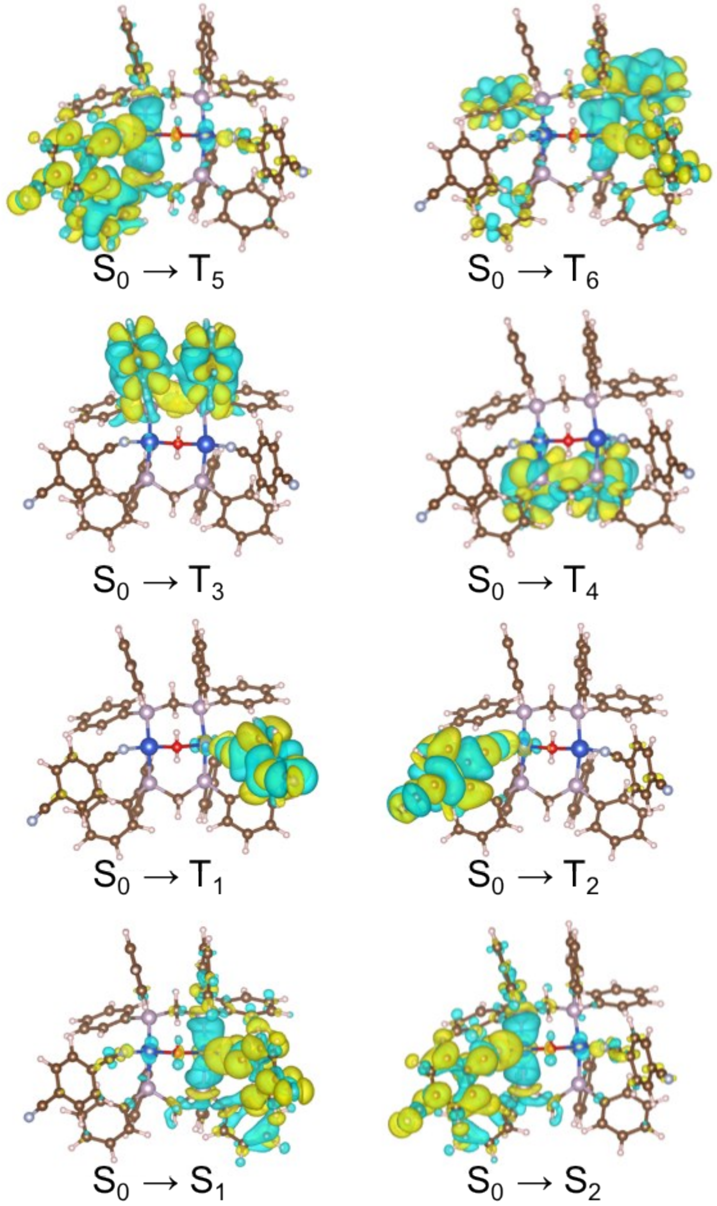

$S_0 \rightarrow T_5$ $S_0 \rightarrow T_6$

$S_0 \rightarrow T_3$ $S_0 \rightarrow T_4$

$S_0 \rightarrow T_1$ $S_0 \rightarrow T_2$

$S_0 \rightarrow S_1$ $S_0 \rightarrow S_2$

**Fig. S18**. Isosurface representations of the electronic charge-density difference between the first vertical singlet ($S_1$, $S_2$) and triplet ($T_1$, $T_2$, $T_3$, $T_4$, $T_5$, $T_6$) excited states and the ground state ($S_0$) (blue = density depletion, greenish = density increase) (± $1.10^{-4}$ e.bohr$^{-3}$).

## V. IR-spectrum of Ddry

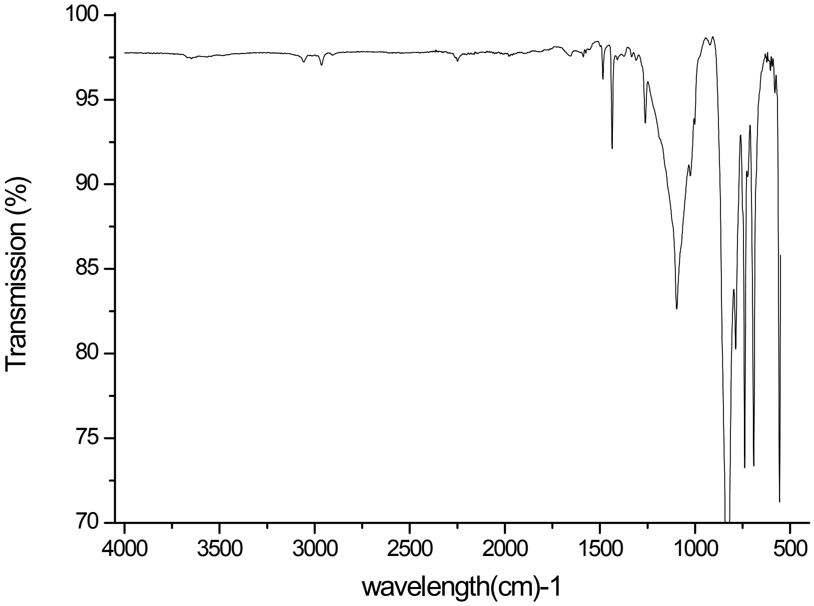

**Fig. S19.** IR spectrum of $\mathbf{D_{dry}}$ in the solid state at 298K

## VI. Preliminary description of the mecanochromic behaviour of $\mathbf{D_{dry}}$: solid state luminescence spectra and power X-ray diagrams obtained after grinding of $\mathbf{D_{dry}}$.

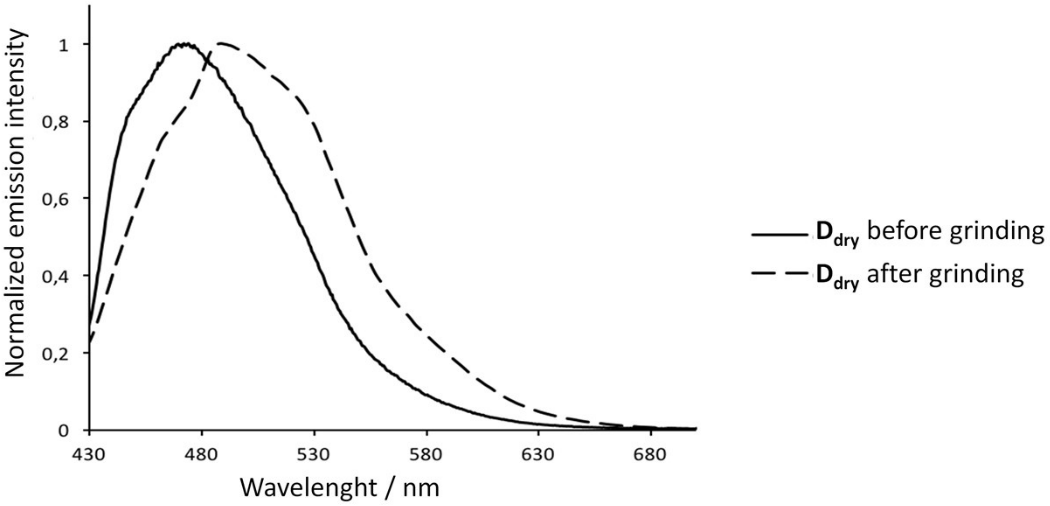

**Fig. S20.** Normalized solid state emission spectra of $\mathbf{D_{THF}}$ before and after grinding.

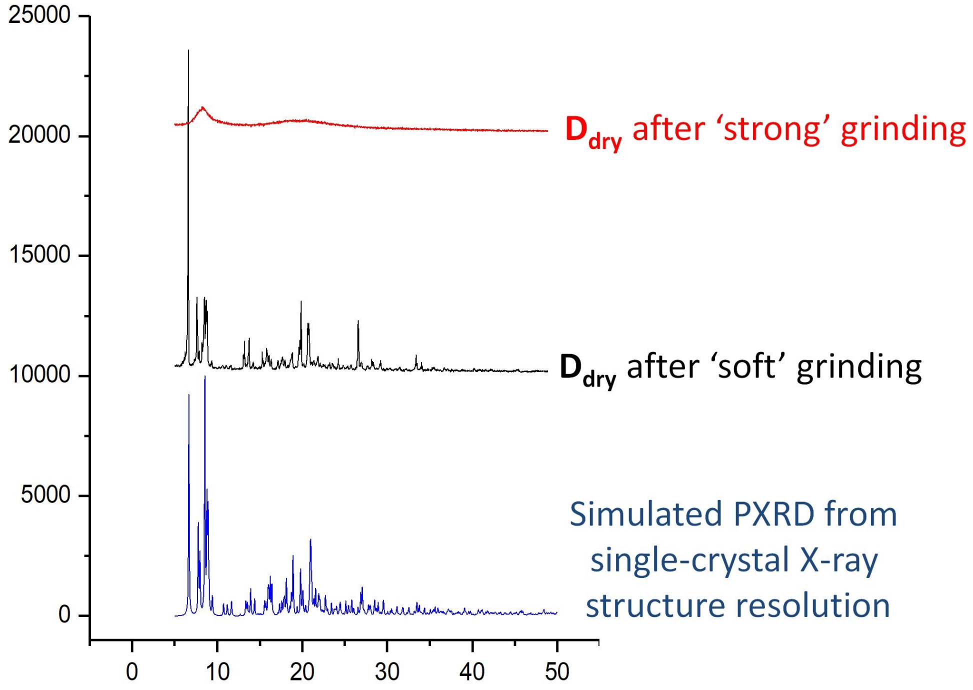

**Fig. S21.** Power X-ray diffraction diagrams of $\mathbf{D_{THF}}$ before and after grinding.

## VII. References for the supplementary information file

[1] Otwinowski, Z.; Minor, W. In *Methods in Enzymology*, (Ed.: C.W. Carter, Jr. & R.M. Sweet), New York:Academic Press**, 1997**, *276*, 307.

[2] Altomare, A.; Burla, M. C.; Camalli, M.; Cascarano, G.; Giacovazzo, C.; Guagliardi, A.; Moliterni, A. G. G.; Polidori, G.; Spagna, R. *J. of Applied Cryst.* **1999***, 32,* 115.

[3] Sheldrick G.M., *SHELX97,* Program for the Refinement of Crystal Structures, University of Göttingen, Germany, **1997**.

[4] (a) Spek, A. L. *J. Appl. Crystallogr.* **2003**, *36*, 13; (b) van der Stuis, P.; Spek, A. L. *Acta Crystallogr.* **1990**, *46*, 194.

[5] International Tables for X-ray Crystallography, vol C, Ed. Kluwer, Dordrech, 1992.

[6] (a) Frisch, M. J.; Trucks, G. W.; Schlegel, H. B.; Scuseria, G. E.; Robb, M. A.; Cheeseman, J. R.; Scalmani, G.; Barone, V.; Mennucci, B.; Petersson, G. A.; Nakatsuji, H.; Caricato, M.; Li, X.; Hratchian, H. P.; Izmaylov, A. F.; Bloino, J.; Zheng, G.; Sonnenberg, J. L.; Hada, M.; Ehara, M.; Toyota, K.; Fukuda, R.; Hasegawa, J.; Ishida, M.; Nakajima, T.; Honda, Y.; Kitao, O.; Nakai, H.; Vreven, T.; Montgomery, Jr., J. A.; Peralta, J. E.; Ogliaro, F.;

Bearpark, M.; Heyd, J. J.; Brothers, E.; Kudin, K. N.; Staroverov, V. N.; Kobayashi, R.; Normand, J.; Raghavachari, K.; Rendell, A.; Burant, J. C.; Iyengar, S. S.; Tomasi, J.; Cossi, M.; Rega, N.; Millam, N. J.; Klene, M.; Knox, J. E.; Cross, J. B.; Bakken, V.; Adamo, C.; Jaramillo, J.; Gomperts, R.; Stratmann, R. E.; Yazyev, O.; Austin, A. J.; Cammi, R.; Pomelli, C.; Ochterski, J. W.; Martin, R. L.; Morokuma, K.; Zakrzewski, V. G.; Voth, G. A.; Salvador, P.; Dannenberg, J. J.; Dapprich, S.; Daniels, A. D.; Farkas, Ö.; Foresman, J. B.; Ortiz, J. V.; Cioslowski, J.; Fox, D. J.; Gaussian 09, Revision A.02; Gaussian Inc.: Wallingford, CT, 2009; (b) Ibid, Gaussian 09, Revision C.01; Gaussian Inc.: Wallingford, CT, 2009.

[7] C. Adamo, V. Barone, J. Chem. Phys., 1999, 6158-69, 110.

[8] A. Schaefer, H. Horn, and R. Ahlrichs, J. Chem. Phys., 1992, 97, 2571-2577. A. Schaefer, C. Huber, and R. Ahlrichs, J. Chem. Phys., 1994, 5829-5835, 100.